Electron spin-echo-detected excitation spectroscopy of manganese-doped $Ba_3(VO_4)_2$: Identification of tetrahedral Mn^{5+} as the active laser center

B. Buijsse and J. Schmidt
Huygens Laboratory, Department of Physics and Astronomy, P.O. Box 9504, 2300 RA Leiden, The Netherlands

I. Y. Chan
Department of Chemistry, Brandeis University, Waltham, Massachusetts 02138

David J. Singel
108 Gaines Hall, Department of Chemistry and Biochemistry, Montana State University, Bozeman, Montana 59717
(Received 29 August 1994)

Electron-spin-echo spectroscopy on the lowest $^3A_2$ state of Mn^{5+} ions in $Ba_3(VO_4)_2$ in combination with pulsed laser excitation at 1176.6 nm proves that the laser activity in this material derives from the $^1E \leftrightarrow {}^3A_2$ transition of the Mn^{5+} ion. This result is corroborated by Zeeman experiments on the $^1E \rightarrow {}^3A_2$ emission line, which further reveal the Zeeman splitting of the ^1E state.

INTRODUCTION

In recent years several potential solid-state-laser materials have been developed that luminesce in the near infrared, and are therefore particularly interesting for use in fiber-optic communication. This development was spurred by the discovery of chromium-doped forsterite ($Cr:Mg_2SiO_4$).[1] The active optical center in this crystal was identified, by a combination of optical Zeeman[2] and electron-paramagnetic-resonance[3] (EPR) spectroscopy, as Cr^{4+}, a $3d^2$ ion, incorporated at tetrahedral sites in the host lattice. This assignment led to an increased interest in analogous Cr^{4+} systems including YAG,[4] Y_2SiO_5,[5] as well as other $3d^2$ ions, in particular Mn^{5+}, which can be doped into a variety of lattices. For instance, Mn^{5+} is well stabilized at tetrahedral sites occurring in phosphates and vanadates.

Materials doped with manganese that have been under examination recently include $Sr_5(PO_4)_3Cl$ and Ca_2PO_4Cl (Ref. 6) and $Ba_5(PO_4)_3Cl$ and Ca_2VO_4Cl.[7] Near-infrared emission was observed in these crystals and it was assigned to the $^1E \rightarrow {}^3A_2$ transition of a Mn^{5+} ion located at tetrahedral sites. More recently $Mn:Ba_3(VO_4)_2$ has been investigated by Merkle *et al.*,[8] who reported a similar optical spectrum. More significantly, they also reported laser oscillation at room temperature under pulsed 592-nm excitation. The stimulated emission occurs at 1181 nm with a threshold of 0.3 J/cm^2. The strong absorption bands and 0.43-ms room-temperature lifetime make this system very promising for flash-lamp or $Al_xGa_{1-x}As$-diode pumping.

In all of these studies the optical center has been identified as a Mn^{5+} ion at a tetrahedral lattice site. Recently however, Whitmore, Verdun, and Singel[9] have shown by EPR spectroscopy that $Mn:Ba_8(VO_4)_2$ laser crystals contain not only Mn^{5+} but also a $S=\frac{3}{2}$ center attributed to Mn^{4+}. The Mn^{4+} centers, also incorporated at the tetrahedral vanadate site, could presumably yield ir laser luminescence. To determine unambiguously whether the Mn^{5+} or Mn^{4+} is the laser active ion we undertook experiments in which electron-spin-echo-(ESE)-detected EPR spectroscopy is combined with optical excitation. In these experiments we use the transient, ESE-detected EPR signal to selectively monitor the Mn^{5+} center. Then, we examine the wavelength-dependent influence of a laser prepulse on the EPR signal intensity. We find unambiguously that the laser action in $Mn:Ba_3(VO_4)_2$ derives from the Mn^{5+} ($3d^2$) ions. We also confirm this result with optical Zeeman spectroscopy, which provides additional insight into the electronic structure of the Mn^{5+} ion in $Ba_3(VO_4)_2$.

THE LOWEST ELECTRONIC STATES IN $Ba_3(VO_4)_2$

$Ba_3(VO_4)_2$ belongs to the space group $R\bar{3}2/m$ and has trigonal symmetry.[10] The trigonal axis is the crystallographic c axis. The crystal consists of discrete vandate tetrahedra that are linked by barium ions. The unit cell contains two tetrahedra which both have one trigonal axis coincident with the c axis. The tetrahedra are slightly distorted by compression along the c axis and the point group of the tetrahedron is C_{3v} instead of T_d. The distortion however is small (0.01 Å on a V-O distance of 1.70 Å) and it is reasonable to assume tetrahedral symmetry in first approximation.

For the description of the lower excited states of the MnO_4^{3-} guest complex we use the molecular-orbital (MO) model of Ballhausen and Liehr for the metal tetroxo anions.[11] The MO's are constructed from $3d$ and $4s$ atomic orbitals (AO's) of Mn^{5+} and from the $2s$ and $2p$ AO's of the four O^{2-} ions. The latter are combined into σ and π orbitals belonging to the irreducible representations (IR's) of T_d.

The two highest occupied MO's are $t_1(\pi)$ and $e(\pi)$. The MO $t_1(\pi)$ exclusively consists of the $\pi(t_1)$ AO's on the O^{2-} ligands. The higher-lying MO $e(\pi)$ is a linear combination of $3d(e)$ AO's ($3d_{z^2}$ and $3d_{x^2-y^2}$) of Mn^{5+} and $\pi(e)$ AO's of O^{2-}. The lowest unoccupied MO is

 ©1995 The American Physical Society

$t_2(\sigma,\pi)$ and is constructed from $3d(t_2)$ AO's $(3d_{xy},3d_{xz},3d_{yz})$ of Mn^{5+} and $\pi(t_2)$ AO's of O^{2-}. Up to $t_1(\pi)$ all the MnO_4^{3-} orbitals are filled with 24 valence electrons of the complex. The two remaining electrons occupy the $e(\pi)$ orbital which is half-filled. The three allowed states which derive from this ground configuration are $^1A_1$, $^3A_2$, and ^1E. Crystal-field theory of a d^2 ion in a tetrahedral field predicts that the $^3A_2$ state is the lowest in energy. The ^1E is the first excited state followed by the $^1A_1$ state.[12]

The lowest excited states which can be obtained by one-electron excitations are those corresponding with the configurations $t_1^6et_2$, $t_1^5e^3$ and $t_1^5e^2t_2$. They result in $^3T_2$ and $^3T_1$ states. $^3T_2$ is the lowest in energy and lies between 10 000 and 12 500 cm^{-1} above the ground state.[8] $^3T_1$ lies between 12 500 and 16 700 cm^{-1} above $^3A_2$. The ^1E state which arises from the e^2-ground configuration lies somewhat below $^3T_2$ and $^3T_1$.

EXPERIMENTAL

The homebuilt, homodyne electron-spin-echo (ESE) spectrometer used in the experiments operates at a frequency of 9.35 GHz.[13] The ESE signal is generated by a $\pi/2$- and π-pulse sequence with pulse lengths of 40 and 80 ns, respectively, and separated by a time interval $\tau=550$ ns. The apparatus allows for alignment of $\mathbf{B}_0$ in any orientation in the crystal frame.

EPR spectra of Mn^{5+} in the $Ba_3(VO_4)_2$ sample were recorded by measuring the electron-spin-echo (ESE) signal following a $\pi/2$-τ-π microwave pulse sequence as a function of the magnetic field $\mathbf{B}_0$. The repetition rate in this experiment is 10 Hz.

In the optically modulated ESE (OMESE) experiments the magnetic field is first tuned to a resonant transition of the Mn^{5+} ion. The intensity of the ESE signal is then monitored as a function of the wavelength of a laser pulse, preceding the $\pi/2$-τ-π microwave pulse sequence by a time $t_d=1$ μs. The spectrum so recorded is called the OMESE spectrum.

The laser prepulse is generated by a Nd:YAG-pumped dye laser in combination with a Raman shifter. This Raman shifter is a tube filled with H_2 gas at a pressure of 40 bar. It produces side bands which are shifted with respect to the incoming dye-laser pump beam by an integer number times the vibrational frequency of 4155 cm^{-1} of H_2. By employing Rhodamine-B in the dye laser and by taking the second Stokes-shifted output of the Raman shifter we obtain output pulses of about 1.3 mJ with a duration of 8 ns, which can be varied between 1110 and 1187 nm by scanning the dye laser.

In addition to the ESE experiments we performed optical Zeeman experiments in the presence of a magnetic field. This magnetic field could be varied between 0 and 5 T and was aligned either with the crystal a or c axis. In this case the sample was irradiated at 700 nm with a cw Ar^+-ion-pumped dye laser with a bandwidth of about 1 cm^{-1}. The luminescence was dispersed by a SPEX 1704 1-m monochromator with a grating blazed at 1000 nm with 1200 lines/mm. The slit width was 20 μm and the height of the slit was 1 mm. The laser beam was amplitude modulated at about 87 Hz by an optical chopper. The detector consisted of a cooled North-Coast Germanium photodetector connected to a lock-in amplifier. All experiments were carried out at a temperature of 1.2 K.

The sample, a single crystal of $Ba_3(VO_4)_2$, was grown by the laser pedestal growth method under an oxidizing atmosphere by Dr. H. Verdún of Fibertek, Inc. The melt contained 0.25 wt % manganese. The color of the sample is aquamarine and its shape is cylindrical with a diameter of 1.5 mm and a length of 4 mm.

RESULTS

In Fig. 1 the ESE-detected EPR spectrum of the $Mn:Ba_3(VO_4)_2$ sample is shown for $\mathbf{B}_0\|c$. The EPR lines consist of six components which are typical for a hyperfine interaction with the ^{55}Mn ($I=\frac{5}{2}$) nuclear spin. Two strong sextets are present at $\mathbf{B}_0=0.137$ T and 0.535 T and a weaker, nominally forbidden transition at $\mathbf{B}_0=0.169$ T typically for a $S=1$ triplet spin system with $g_\parallel=1.9608, g_\perp=1.9722$ and a zero-field splitting parameter $|D|=5.81$ GHz. These parameters are in agreement with the values reported earlier by Whitmor, Verdun, and Singel[9] for Mn^{5+}. Note however that the signal of Mn^{4+} observed by these authors around $g=2$ is almost unobservable in our spectrum. We think that this is related to our ESE detection protocol which is much less sensitive for rapidly relaxing spin systems.

The relation between the Mn^{5+} ion and the reported emission line at 1181 nm was probed by an ESE-detected optical excitation experiment. We subject the crystal to the pulsed output of the laser system and monitor the ground-state ESE signal as a function of the excitation wavelength. A change in the ground-state triplet sublevel population by resonant optical excitation alters the echo height. We tuned the magnetic field to a hyperfine component of the high-field EPR transition with $\mathbf{B}_0\|c$ to produce the two-pulse ESE signal. Then we applied a vari-

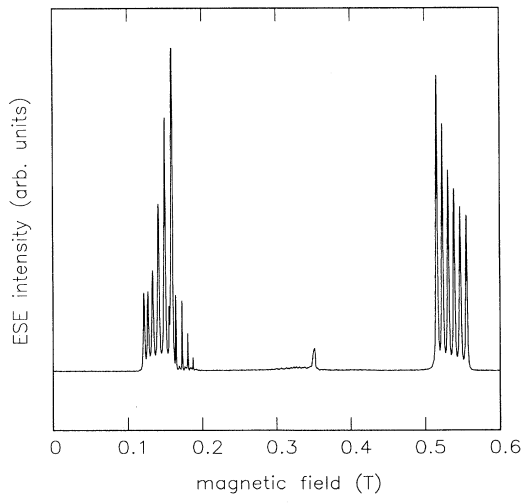

FIG. 1. The ESE-detected EPR spectrum of $Mn:Ba_3(VO_4)_2$ with $\mathbf{B}_0\|c$.

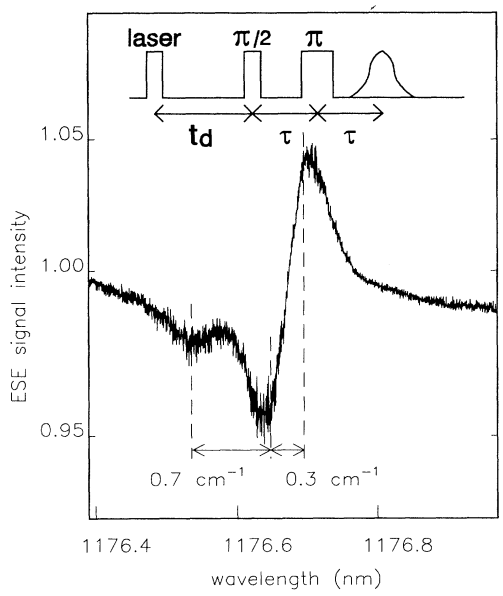

FIG. 2. The ESE-detected EPR signal intensity as a function of the wavelength of the excitation laser. The value 1.00 along the vertical axis indicates the echo intensity without the preceding laser pulse, $\mathbf{B}_0 \| c$.

able wavelength laser prepulse before the microwave pulse sequence (see Fig. 2). The OMESE spectrum obtained by monitoring the echo signal as a function of the laser wavelength is displayed in Fig. 2.

The spectrum in Fig. 2 shows a remarkable structure. Starting at low wavelength we first see a small decrease in intensity, then a larger decrease and finally an increase to a level which even exceeds the echo intensity without laser excitation. The change in amplitude is of the order of 5%. The spacing of the three lines is 0.3 and 0.7 cm^{-1}, respectively, whereas the width of the lines is 0.66 cm^{-1}. By scanning the excitation wavelength over a

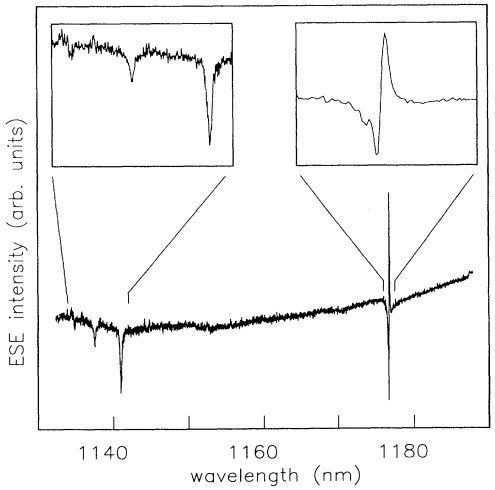

FIG. 3. The ESE-detected EPR signal intensity as a function of the wavelength of the excitation laser recorded in a wavelength region larger than in Fig. 2.

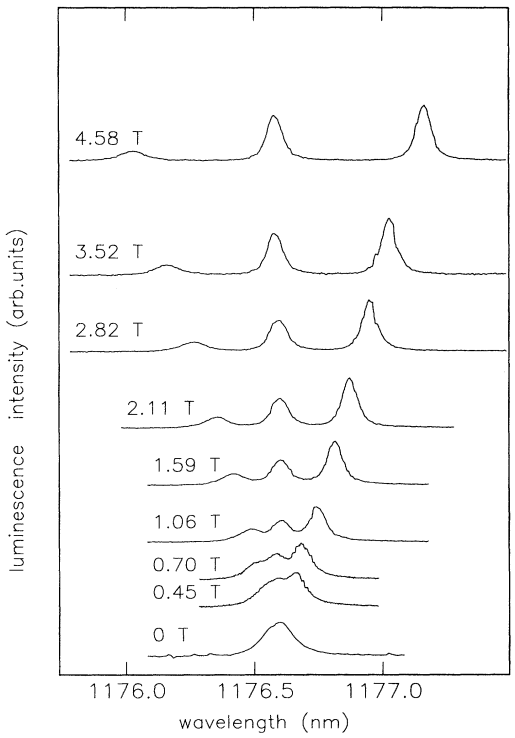

FIG. 4. The emission spectrum of $Mn:Ba_3(VO_4)_2$ recorded for several values of the applied magnetic field $\mathbf{B}_0 \perp c$.

broader wavelength region three additional (negative) peaks at 1134.8 1137.5, and 1141.0 nm were observed (see Fig. 3). They correspond to an energy shift with respect to the 1176.6-nm signal of 313, 292, and 265 cm^{-1}, respectively.

We note that the center of the OMESE spectrum in Fig. 2 is at 1176.6 nm, significantly different from the wavelength of 1181 nm reported for the emission of $Mn:Ba_3(VO_4)_2$.[8] We calibrated our laser wavelength via a monochromator with a neon calibration lamp and

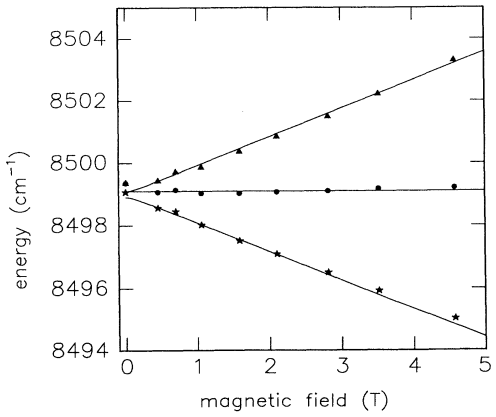

FIG. 5. The splitting of the emission line in $Mn:Ba_3(VO_4)_2$ with $\mathbf{B}_0 \perp c$ as a function of the intensity of the applied magnetic field. The solid lines represent the calculated splittings with $D = -5.81$ GHz and $g_\perp = 1.9722$.

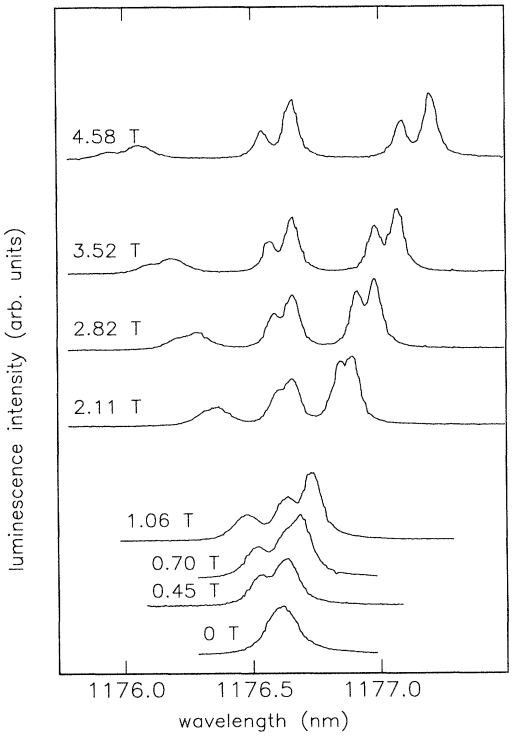

FIG. 6. The emission spectrum of $Mn:Ba_3(VO_4)_2$ recorded for several values of the applied magnetic field $\mathbf{B}_0 \| c$.

confirmed that our observed wavelength of excitation is precise within 0.2 cm^{-1}. Simultaneously we determined the bandwidth of the laser as being about 0.25 cm^{-1}.

To elucidate the difference between the emission wavelength of 1176.6 nm found by us and that reported in the literature[8] we decided to measure also the emission spectrum of our $Mn:Ba_3(VO_4)_2$ sample. This emission spectrum was recorded in zero field as well as in the presence of a magnetic field up to 4.58 T. In Fig. 4 the spectrum is shown with $\mathbf{B}_0 \perp c$. In zero field a single emission line is present at 1176.6 nm which splits almost linearly with the applied magnetic field (see Fig. 5). The width of the lines in Fig. 4 at $\mathbf{B}_0 = 5.48$ T are 0.80, 0.53, and 0.50 cm^{-1}, respectively, starting from the left side. For $\mathbf{B}_0 \| c$ an additional splitting on each of these lines is visible (see Fig. 6). The corresponding diagram in Fig. 7 shows that this additional splitting is also linear with the magnetic field.

DISCUSSION

It is clear that the centers of the emission with $\mathbf{B}_0 = 0$ in Figs. 4 and 6 and of the absorption line in the excitation spectrum of Fig. 2 coincide within 0.1 nm, at the value of 1176.6 nm. These lines are related to the $^1E \leftrightarrow {}^3A_2$ transition of Mn^{5+}. First we consider the shape of the ESE-detected excitation spectrum. This shape can be explained if we assume that the laser selectively excites population from the Zeeman sublevels of the $^3A_2$ ground-state to the ^1E state of Mn^{5+} (see Fig. 8). Excitation from the upper Zeeman level (longest wavelength) gives rise to an increase in the population difference between the upper two levels which are in resonance with the pulsed microwaves. The observed echo intensity is proportional to this population difference and consequently will also increase. Excitation from the middle level has the opposite effect and causes a decrease in intensity. Excitation from the lowest level gives rise to a decrease of the population difference of the upper two levels by a spin-lattice relaxation process which restores the Boltzmann distribution. The result is a decrease of the ESE signal intensity. We note that this analysis is based on the assumption that the zero-field splitting parameter $D < 0$ in the $^3A_2$ ground state. The distances between the peaks of 0.3 and 0.7 cm^{-1} are in excellent agreement with the values calculated for the separation of the Zeeman levels in the applied magnetic field of 0.561 T parallel to the crystal c axis and with $D = -5.81$ GHz $= -0.19$ cm^{-1}.

It is remarkable that the Zeeman splitting of the $^3A_2$ ground state is visible in the excitation spectrum (see Fig. 2), which is taken in a magnetic field of only 0.561 T.

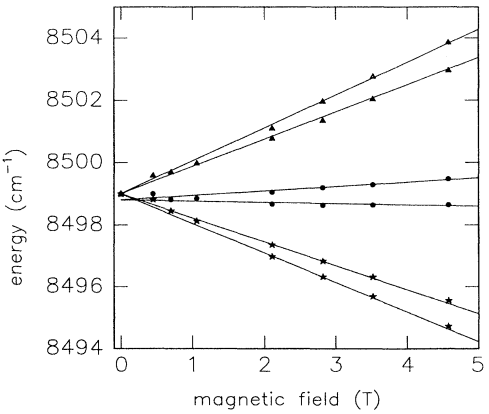

FIG. 7. The splitting of the emission line in $Mn:Ba_3(VO_4)_2$ with $\mathbf{B}_0 \| c$ as a function of the intensity of the applied magnetic field. The solid lines represent the calculated splittings with $D = -5.81$ GHz and $g_\parallel = 1.9608$ and $\langle L_z \rangle = (0.39 \pm 0.01)$.

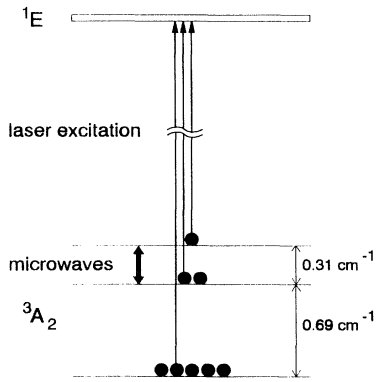

FIG. 8. A schematic representation of the pulsed-laser excitation from the $^3A_2$ ground state to the ^1E excited state of the Mn^{5+} ion in $Ba_3(VO_4)_2$ in the presence of a magnetic field of 0.561 T parallel to the crystal c axis.

This indicates that the $^1E \leftrightarrow {}^3A_2$ transition is very narrow, in the order of 0.7 cm^{-1}. The results of the emission experiments are in agreement with this estimate. For instance in a magnetic field of 0.7 T the Zeeman splitting of the $^3A_2$ ground state is also visible in the emission (see Fig. 4). Presumably this narrow linewidth reflects the fact that the optical transition occurs within the e^2-electronic configuration which is relatively insensitive to lattice distortions.

The three additional negative peaks in the ESE-detected excitation spectrum of Fig. 3 at wavelengths shorter than 1176.6 nm are assigned to transitions to vibronic levels, a suggestion which is mainly based on the size of the frequency interval. A tetrahedral molecule has four vibrational frequencies which can be classified according to the IR's of T_d. Two the vibrational modes transform as the T_2 representation, one as A_1 and one as the E representation.[14] In the crystal discrete, isolated VO_4^{3-} and guest MnO_4^{3-} are present. If the vibrations are localized on these tetrahedra, energies of the order of several hundred wave numbers are expected. Kingsley, Prener, and Segall[12] found for the E mode (which is a bending mode) of MnO_4^{3-} doped in Ca_2PO_4Cl a value of 245 cm^{-1} and for PO_4^{3-}, 363 cm^{-1}. More recently Herren *et al.*[7] studied MnO_4^{3-} doped in various phosphates and vanadates. For MnO_4^{3-} doped in vanadate crystals they found a value of roughly 310 cm^{-1}, and 350 cm^{-1} for MnO_4^{3-}-doped phosphate crystals. These vibrational modes can show a fine splitting due to lattice vibrations of the order of ten wave numbers. We tentatively assign the line at 265 cm^{-1} above the ^1E state to an E mode of MnO_4^{3-}, while the two lines at 292 and 313^{-1} cm^{-1} could correspond to the 265-cm^{-1} vibration coupled with lattice vibrations. The fact that the three lines are broader than the vibrationless $^1E \leftarrow {}^3A_2$ transition is attributed to the short lifetime of the vibrationally excited states.

The field-dependent emission spectra further confirm the results of the ESE-detected excitation experiments and moreover give us information about the zero-field splitting and the orbital angular momentum of the ^1E state. With $\mathbf{B}_0 \perp c$ we can easily distinguish the transitions from ^1E to the three Zeeman components of the $^3A_2$ ground state (see Fig. 4). This again indicates that the width of these levels is less than 1 cm^{-1}. From the asymmetry in the Zeeman splittings (Fig. 5) we also derive that the zero-field splitting parameter $D<0$ in the $^3A_2$ ground state. With $\mathbf{B}_0 \| c$ the field couples to an orbital angular momentum L_z associated with the ^1E state. As a result this twofold degenerate state will undergo an orbital Zeeman splitting and since emission from these two sublevels to the three Zeeman components of the $^3A_2$ ground state is allowed we observe an additional splitting in the spectra. This additional splitting enables us to calculate the expectation value of the orbital angular momentum L_z. Using the expression $\pm g_l \mu_b B \langle L_z \rangle$ with $g_l=1$, for the shift of the levels we find $\langle L_z \rangle = (0.39 \pm 0.01)$. In the simplified situation, in which we only consider the d_{z^2} and $d_{x^2-y^2}$ AO's of the Mn ion, we expect to find a value equal to zero. The fact that we observe a nonzero value for the angular momentum shows that spin-orbit coupling with excited $^3T_1$ and $^3T_2$ states which are near in energy should be considered. In addition, we have to take into account the vibronic Jahn-Teller interaction which leads to a reduction of the angular momentum because it couples the electronic and vibronic wave function. In our particular case we deal with the so-called $E \otimes e$ Jahn-Teller problem with E the representation of the electronic wave function and e the representation of the vibronic wave function. The lowest energy state in this coupled representation is again an E state for which the expectation value of the orbital angular momentum is $P_{\text{nucl}} \langle \phi_{\text{el}} | L_z | \phi_{\text{el}} \rangle$. Here P_{nucl} is called the orbital reduction factor which depends only on the nuclear part of the mixed wave function. Without further knowledge it is not possible to calculate the precise value of P_{nucl} which lies between 0 and 1.[15]

Finally we remark that the zero-field splitting of the ^1E state is exceptionally small (smaller than 0.1 cm^{-1}). A splitting of the ^1E state arises when the symmetry is lower than C_{3v}. For instance, in Mn:Ca_2VO_4Cl the average deviation of the six O-Mn-O angles of the regular tetrahedron value of 109.5° is 6.9° and the orbital splitting is 363 cm^{-1}.[16] In our Mn:$Ba_3(VO_4)_2$ system the actual symmetry of the MnO_4^{3-} tetrahedron is almost perfectly C_{3v}. Therefore it is not unreasonable that the orbital splitting is close to zero. On the other hand it is not excluded that a dynamic Jahn-Teller effect averages the splitting to zero.

CONCLUSION

The results of the experiments demonstrate that the laser emission observed in Mn:$Ba_3(VO_4)_2$ at 1176.6 nm is related to the presence of Mn^{5+} ($3d^2$) ions, which substitute into the lattice at the vanadium site. The ESE-detected excitation spectra show that the EPR signals, originating from Mn^{5+}, correspond to the optical transition between the $^3A_2$ ground state and the ^1E excited state of this ion. This conclusion is further confirmed by the Zeeman effect on the emission line. The latter experiment allows us not only to observe the Zeeman splitting in the $^3A_2$ ground state but also to determine the value of the orbital angular momentum associated with the excited ^1E state. An interesting finding is that the ^1E state shows a zero-field splitting close to zero (<0.1 cm^{-1}). This is not unreasonable in view of the small distortion of the MnO_4^{3-} tetrahedron.

ACKNOWLEDGMENTS

Support of this work by the Army Research Office (DAAL 03-90-0113) and helpful conversations with Dr. A. Pinto are gratefully acknowledged. I. Y. Chan is grateful for the support of the National Science Foundation (CHE-9306931). The crystal of Mn-doped $Ba_3(VO_4)_2$ was kindly supplied by Dr. Horacio Verdún. The work performed in Leiden forms part of the research program

of the "Stichting voor Fundamenteel Onderzoek der Materie (FOM)" and has been made possible with financial support from the "Nederlandse Organisatie voor Wetenschappelijk Onderzoek (NWO)". The authors wish to thank Professor J. H. van der Waals for fruitful discussions and Dr. J. W. A. Coremans for valuable assistance during the ESE experiments.

[1]V. Petričevic, S. K. Gayen, R. R. Alfano, K. Yamagishi, H. Anzai, and Y. Yamaguchi, Appl. Phys. Lett. **52**, 1040 (1988); V. Petričevic, S. K. Gayen and R. R. Alfano, *ibid.*, **53**, 2590 (1988); H. R. Verdun, L. M. Thomas, D. M. Andrauskas, T. McCollum, and A. Pinto, *ibid.* **53**, 2593 (1988).

[2]T. S. Rose, R. A. Fields, M. H Whitmore, and D. J. Singel, J. Opt. Soc. Am. B **11**, 428 (1994); W. Jia, H. Liu, S. Jaffe, W. M. Yen, and B. Denker, Phys. Rev. B **43**, 5234 (1991).

[3]M. H. Whitmore, A. Sacra, and D. J. Singel, J. Chem. Phys. **98**, 3656 (1993).

[4]N. B. Angert, N. I. Borodin, V. M. Garmash, V. A. Zhitnyuk, A. G. Okhrimchuk, O. G. Siyuchenko, and A. V. Shestakov, Sov. J. Quantum Electron. **18**, 73 (1988).

[5]B. H. T. Chai, Y. Shimony, C. Deka, X. X. Zhang, E. Munin, and M. Bass, in *OSA Proceedings on Advanced Solid-State Lasers,* edited by L. L. Chase and A. A. Pinto (Optical Society of America, Washington, DC, 1992), Vol. 13, p. 28.

[6]J. A. Capobianco, G. Cormier, R. Moncorgé, H. Manaa, and M. Bettinelli, Appl. Phys. Lett. **60**, 163 (1992).

[7]M. Herren, H. U. Güdel, C. Albrecht, and D. Reinen, Chem. Phys. Lett. **183**, 98 (1991).

[8]L. D. Merkle, A. Pinto, H. R. Verdun, and B. McIntosh, Appl. Phys. Lett. **61**, 2386 (1992).

[9]M. H. Whitmore, H. R. Verdun, and D. J. Singel, Phys. Rev. B **47**, 11 479 (1993).

[10]P. Süsse and M. J. Buerger, Z. Kristallogr. **131**, 161 (1970).

[11]C. J. Ballhausen and A. D. Liehr, J. Mol. Spectrsc. **2**, 342 (1958).

[12]J. D. Kingsley, J. S. Prener, and B. Segall, Phys. Rev. **137A**, 189 (1965).

[13]W. A. J. A. van der Poel, D. J. Singel, J. Schmidt, and J. H. van der Waals, Mol. Phys. **49**, 1017 (1983).

[14]G. Herzberg, *Molecular Spectrscopy and Molecular Structure* (D. Van Nostrand, Princeton, NJ, 1945), Vol. II, p. 139.

[15]F. S. Ham, in *Electron Paramagnetic Resonance,* edited by S. Geschwind (Plenum, New York, 1972), p. 33.

[16]M. Herren, T. Riedner, H. U. Güdel, C. Albrecht, U. Kaschuba, and D. Reinen, J. Lumin. **53**, 452 (1992).